



Published in final edited form as:

Cancer Immunol Res. 2020 March ; 8(3): 309–320. doi:10.1158/2326-6066.CIR-19-0293.

Glypican-3-specific CAR T cells co-expressing IL15 and IL21 have superior expansion and antitumor activity against hepatocellular carcinoma

Sai A Batra¹, Purva Rathi¹, Linjie Guo¹, Amy N Courtney¹, Julien Fleurence¹, Julien Balzeau¹, Rahamthulla S. Shaik¹, Thao P Nguyen¹, Meng-Fen Wu², Shaun Bulsara², Maksim Mamonkin³, Leonid S Metelitsa^{1,3}, Andras Heczey^{1,3,4}

¹Texas Children's Cancer Center, Department of Pediatrics, Baylor College of Medicine

²Dan L Duncan Cancer Center Biostatistics Shared Resource, Baylor College of Medicine

³Center for Cell and Gene Therapy, Baylor College of Medicine

⁴Texas Children's Hospital Liver Tumor Center, Houston, TX, 77030

Abstract

Hepatocellular carcinoma (HCC) is the fourth most common cause of cancer-related death in the world and curative systemic therapies are lacking. Chimeric antigen receptor (CAR)-expressing T cells induce robust antitumor responses in patients with hematologic malignancies but have limited efficacy in patients with solid tumors including HCC. IL15 and IL21 promote T cell expansion, survival and function, and can improve the antitumor properties of T cells. We explored whether transgenic expression of IL15 and/or IL21 enhanced glypican-3-CAR (GPC3-CAR) T cells' antitumor properties against HCC. We previously optimized the co-stimulation in GPC3-CARs and selected a second generation GPC3-CAR incorporating a 4-1BB costimulatory endodomain (GBBz) for development. Here, we generated constructs encoding IL15, IL21, or both with GBBz (15.GBBz, 21.GBBz, and 21.15.GBBz, respectively) and examined the ability of transduced T cells to kill, produce effector cytokines, and expand in an antigen-dependent manner. We performed gene expression and phenotypic analyses of GPC3-CAR T cells and CRISPR-Cas9 knock-out of the *TCF7* gene. Finally, we measured GPC3-CAR T cell antitumor activity in murine xenograft models of GPC3+ tumors. The increased proliferation of 21.15.GBBz T cells was at least in part dependent on upregulation and maintenance of TCF-1 (encoded by *TCF7*) and associated with a higher percentage of stem cell memory and central memory populations after manufacturing. T cells expressing 21.15.GBBz had superior *in vitro* and *in vivo* expansion and persistence, and the most robust antitumor activity *in vivo*. These results provided preclinical evidence to support the clinical evaluation of 21.15.GPC3-CAR T cells in patients with HCC.

Corresponding author: Andras Heczey, Section Pediatric Hematology and Oncology, Department of Pediatrics, Baylor College of Medicine; 1102 Bates Ave, C.1760.10, Houston, TX 77030; Tel: (832) 824-4233, Fax: (832) 825-4846; axheczey@txch.org.

Conflict of interest disclosure statement:

SAB, PR, LSM and AH have pending patent applications covering GPC3-CARs. Other co-authors report no conflict of interest.

Keywords

IL15; IL21; glypican-3; CAR T cells; hepatocellular carcinoma

Introduction

Hepatocellular carcinoma (HCC) is the fourth most common cause of cancer-related death in the world (1). Lack of curative therapies for unresectable and/or metastatic disease, which occurs in the majority of newly diagnosed cases, results in dismal prognoses (1). Chimeric antigen receptor (CAR)-expressing T cells show clinical successes for the treatment of CD19-positive hematological malignancies (2–6). In contrast, CAR T cells demonstrate only modest antitumor activity in patients with solid tumors, including HCC, in part due to their limited expansion and persistence (7–12). As the overall therapeutic efficacy of CAR T cells strongly correlates with their expansion and persistence in patients with CD19-positive malignancies (2,4), translational approaches to enhance these properties may improve the antitumor efficacy of CAR T therapy in patients with HCC.

Human interleukin 15 (IL15) and IL21 are required for optimal T cell activation, expansion, differentiation, and function (13,14). These cytokines are absent in the HCC microenvironment, depriving T cells of survival signals (13,14). In preclinical models of CD19+ malignancies, neuroblastoma or gliomas, CAR T cells co-expressing either IL15 or IL21 controlled tumors significantly better than CAR T cells alone (15–18). Additionally, IL15 and IL21 can synergistically promote antigen-dependent T cell expansion and cytolytic function (19,20). However, whether IL-15, IL21, or their combined expression enhance the antitumor effector function of CAR T cells against HCC remains unknown. We previously systematically evaluated the *in vitro* and *in vivo* activity of T cells expressing CARs targeting glypican-3 (GPC3), an antigen expressed in over 70% of HCCs but not in non-malignant tissues (21–27). We selected the GPC3-CAR containing a 4-1BB costimulatory endodomain — ‘GBBz’ — for further clinical development, as this receptor induces favorable T_H1-polarized effector cytokine release upon tumor cell engagement and produced superior expansion and antitumor activity (27). Here, to determine the impact of IL15 and IL21 on T cell survival, persistence, and antitumor activity in preclinical models of HCC, we co-expressed IL15, IL21, or both with the GBBz GPC3-CAR in T cells.

We demonstrated that GBBz GPC3-CAR T cells co-expressing IL15 and/or IL21 specifically and effectively killed GPC3-positive tumor cells, including HCC, in an antigen-dependent manner. Our results also indicated that constitutive transgenic expression of both IL15 and IL21 together enriched for less differentiated T cells, which were better protected from apoptosis during repeated exposures to tumor cells. We showed that combined IL15 and IL21 expression maintained the expression of T cell factor –1 (TCF-1), a transcription factor critical for T cell development and survival. CRISPR-Cas9 mediated knock-out of *TCF7* (the gene encoding TCF-1) in IL15 and IL21 co-expressing GPC3-CAR T cells eliminated the improvement in proliferative capacity. Finally, GPC3-CAR T cells co-expressing IL15 and IL21 exhibited the most robust peak expansion and sustained persistence *in vivo* and mediate superior tumor control and survival of HCC tumor-bearing

mice compared to either cytokine alone or controls. These results provided a strong rationale to evaluate IL15 and IL21 co-expressing GBBz CAR in patients with liver tumors (NCT02932956; NCT02905188).

Materials and Methods

Cell lines

The HCC cell line Hep3B, rhabdoid tumor cell line G401, lung carcinoma cell line A549, and human embryonic kidney cell line 293T were obtained from the American Type Culture Collection (ATCC, Manassas, VA) and were cultured in Dulbecco's Modified Eagle Media with 10% fetal bovine serum (FBS) except for 293T cells which were cultured in Iscove Modified Dulbecco Media with 10% FBS. Cells were kept in culture for less than three weeks for any given experiment. Cells were not re-authenticated in the past year. Cells were regularly tested and were negative for Mycoplasma contamination. The HCC cell line Huh-7 was a kind gift from Dr. Xiao-Tong Song (Baylor College of Medicine, Houston, TX) and was maintained in Dulbecco's Modified Eagle Medium and its identity was confirmed at the Characterized Cell Line Core Facility at MD Anderson Cancer Center (Houston, TX) short-tandem repeat method. Cell lines were obtained between 2014–2015. A549-GPC3 cells were generated by transducing A549 cells with a retroviral vector encoding GPC3; Huh-7 firefly luciferase (Ffluc) cells were similarly generated using an eGFP.Ffluc construct (27).

Generation of retroviral constructs

The codon optimized minigene encoding cytokines IL21, IL15, and the GPC3-CAR 'GBBz' (27) linked with a T2A sequence and flanked by NcoI and MluI restriction enzyme sites was synthesized using the GeneArt[®] system (Thermo Fisher Scientific, Waltham, MA). This fragment was subcloned into the pSFG retroviral vector yielding the 21.15.GBBz retroviral construct (Fig. 1A). 21.GBBz was generated from 21.15.GBBz by PCR amplifying genes encoding IL21(F: ATCCTCTAGACTGCCATGGAACGGATC / R: CGTCCCTCGGCTCTAGAATCTTCG) and GBBz (F: TAGAGCCGAGGGACGGGGCT / R: ATGATGACGCGTTAATCATCTGGGGG), followed by In-Fusion[®] cloning (Cat. #: 638920, Takara Bio, Mountain View, CA) into the pSFG retroviral vector backbone according to the manufacturer's manual (Fig. 1A). 15.GBBz was similarly generated by amplifying the gene fragment encoding both IL15 and GBBz (F: ATCCTCTAGACTGCCATGAGAATCAGCAAGCCCC / R: ATGATGACGCGTTAATCATCTGGGGG) and subsequent In-Fusion[®] cloning (Fig. 1A). The 21.15 construct was produced by PCR amplifying the fragment encoding both IL21 and IL15 from 21.15.GBBz (F: ATCCTCTAGACTGCCATGGAACGGATC / R: CAGTGCGCCGCTCAGGCCCTGCTGGTGTT) and in the process generating NcoI and NotI restriction enzyme sites in the introduced 5' and 3' overhangs. This fragment was cloned into a pSFG plasmid bearing the orange monomeric derivative of DsRed fluorescent protein (28). Sequencing was performed following each cloning step to confirm the correct alterations were made (Epoch Life Science, Sugar Land, TX). A CD19-specific CAR (FMC63 scFv, CD28 and 4-1BB costimulatory domains, CD3 ζ signaling endodomain) was used as negative control (29).

Retrovirus production and transduction of primary T cells and cell lines

Transient transfection of HEK 293T cells with plasmids for GPC3-CAR constructs, RDF plasmid encoding the RD114 envelope and PegPam3 plasmid encoding the MoMLV gag-pol was used to generate retroviral supernatants as previously described (30). OKT-3/CD28 mAb-coated plates were used to stimulate human peripheral blood mononuclear cells isolated from healthy volunteer donors (Gulf Coast Regional Blood Center, Houston, TX). After 48h, cells were washed and replated in complete RPMI medium and maintained in incubators at 37C with 5% CO₂ (27).

Cytotoxicity assay

Cytotoxicity of GPC3-CAR T cells was assessed as described previously (27) using a standard four-hour chromium 51 (⁵¹Cr) release assay. Briefly, target cells were labeled with ⁵¹Cr for 1 hour followed by incubation with effector cells for four hours at 37°C using multiple effector-to-target ratios. Cell culture supernatants were collected, and radioactivity was measured in a gamma counter (PerkinElmer, Waltham, MA).

Measurement of cytokines and chemokines

The Human IL15/IL21 ELISA MAXTM Deluxe kit (Biolegend, San Diego, CA) was used to measure IL15 and IL21 concentrations according to the manufacturer's instructions. Briefly, 0.5×10^6 resting CAR T cells were cultured in the presence or absence of Huh-7 cells at a 1:1 ratio. Cell culture supernatants were collected at 72 hours, centrifuged, and frozen until the time of assay. Multiplex cytokine/chemokine immunoassays were performed as previously described using the MILLIPLEX MAP human cytokine/chemokine magnetic bead kit (EMD Millipore, Billerica, MA; Cat #: HCYTOMAG-60K) according to the manufacturer's instructions (27).

To assess the production of IL1b and IL6, monocytes negatively selected from human PBMCs by Pan monocyte isolation kit (Miltenyi Bio130-096-537 kit) were plated at 2.5 : 2.5 : 1 tumor, CAR T cell and monocyte ratio, respectively. Monocyte purity was confirmed by FACS and was above 95% for each co-culture experiments. Supernatants were collected at 20hrs and evaluated with IL1b and IL6 ELISA kits (Biolegend, Cat #: 437005 and R&D Systems, Cat # D6050 respectively) according to the manufacturers manual.

Flow cytometry

GPC3-CAR expression was detected using the anti-F(ab)₂ Alexa Fluor[®] 647-conjugated antibody (Jackson ImmunoResearch) and anti-goat IgG₁ isotype control (Jackson ImmunoResearch, West Grove, PA). The following antibodies were used for T cell phenotyping analyses: anti-CD4-APC/Fire 750 (BioLegend), anti-CD8-V500 (BD Biosciences, San Jose, CA), anti-CD45RO-PE/Cy7 (BioLegend), anti-CD62L-AF488 (BioLegend), anti-CD19-PerCP/Cy5.5 (CCR1; BioLegend), anti-CD3-PE (BD Biosciences), anti-CD279-PerCP/Cy5.5 (PD-1; BioLegend), anti-CD223-PE/Cy7 (LAG-3; BioLegend) and anti-CD366-BV421 (TIM-3; BD Biosciences). Anti-bovine IgG (Sigma-Aldrich, St. Louis, MO) was used to block non-specific binding of other murine antibodies following CAR staining. Flow cytometry assessment was performed on either an LSR-II (BD Biosciences) or iQue Screener PLUS (Intellicyt Corporation, Albuquerque, NM). Results

were analyzed using FlowJo software (FlowJo, Ashland, OR). To detect intracellular TCF-1 expression, CAR T cells were first stained for surface expression of CAR, CD4, and CD8 using the antibodies listed above, followed by staining with anti-TCF1-PE (TCF7, BioLegend) used in conjunction with the True-Nuclear™ Transcription Factor Buffer Set (BioLegend) according to the manufacturer's instructions.

Repeat stimulation stress test

In vitro expansion and persistence were assessed by repeatedly co-culturing CAR T cells with fresh Huh-7 tumor cells every 3–4 days at a 1:1 ratio. At the end of each co-culture interval, CAR T cell counts were measured by flow cytometry staining for the CAR and using CountBright™ beads (ThermoFischer, Waltham, MA; Cat #: C36950) according to manufacturer's instructions. Annexin V staining was performed to assess CAR T cell viability two days after each stimulation using the ApoScreen® Annexin V Apoptosis Kit (SouthernBiotech, Birmingham, AL; Cat #: 10010-09) according to the manufacturer's instructions.

Gene expression profiling

CAR T cells were sorted using a Sony SH800Z instrument (Sony Biotechnology, San Jose, CA) and expanded for one week in complete RPMI supplemented with 100 units/ml penicillin, 100µg/ml streptomycin, and 0.25 µg/ml amphotericin B (ThermoFischer Scientific). Sorted CAR T cells were co-cultured with tumor cells at a 2:1 (E:T) ratio for three days. To confirm the absence of tumor cells prior to RNA extraction, co-cultured cells were analyzed by flow cytometry and the absence of residual tumor cells was confirmed. RNA was extracted using the RNeasy Mini Kit (Qiagen, Germantown, MD; Cat #: 74104) as per the manufacturer's protocol and measured at the Genomic and RNA Profiling Core at Baylor College of Medicine (BCM) using the nCounter Analysis System (NanoString Technologies, Seattle, WA) and the pre-defined nCounter Human Immunology V2 panel (Cat #: XT-CSO-HIM2-12). Gene expression data were normalized and analyzed using nSolver software (NanoString Technologies). Benjamini-Hochberg correction was used for multiple comparisons.

CRISPR-Cas9 mediated *TCF7* knock-out

We screened six *TCF7*-specific sgRNAs and based on their efficiency to knock out *TCF7* (resulting in diminished expression of TCF1, the protein encoded by the gene) measured by FACS selected two sgRNAs targeting the *TCF7* gene locus (target sequences GGGGTCCACTTACCAGCGGGG and GAGCTCGCCAGGTTCGCGCTCGG) for subsequent experiments. sgRNA design and *TCF7* gene disruption in primary activated T-cells was performed as previously described (31).

In vivo experiments

All mice used in this study were maintained at the Small Animal Core Facility of Texas Children's Hospital and handled under protocols approved by the BCM Institutional Biosafety Committee and Institutional Animal Care and Use Committee. Tumor cells or CAR T cells were diluted in 100 µl normal saline and were injected via indicated routes.

In vivo antitumor activity of infused CAR T cells and mouse survival were evaluated in murine HCC xenograft models as described previously (27) with modifications. Briefly, 12-week-old female NOD.Cg-Prkdc^{scid} Il2rg^{tm1Wjl}/SzJ (NSG, The Jackson Laboratory, Bar Harbor, ME) mice were injected intraperitoneally (ip) with 2×10^6 Ffluc+ Huh-7 cells or 5×10^6 Ffluc+ G401 cells followed by 0.5×10^6 or 2×10^6 CAR T cells in 100 μ l normal saline intravenously (iv) via tailvein one or two weeks later, as indicated. Mice were assessed daily and tumor bioluminescence was measured after iv injection of luciferin using the IVIS Lumina III imaging system (PerkinElmer, Waltham, MA).

To evaluate CAR T cell *in vivo* proliferation and persistence, mice were injected with 2×10^6 Huh-7 cells ip followed two weeks later by iv injection of 2×10^6 CAR T cells co-expressing an optimized *Ffluc* (32). Mice were imaged every other day following CAR T cell injection to monitor expansion. Blood and spleens were collected on days 15 and 18, respectively, and evaluated for the presence of CAR T cells by flow cytometry. All animals were sacrificed according to institution standards prior to harvesting spleens. Cells were stained for mouse CD45 using anti-mouse CD45-PE or PerCP/Cy5.5 (both BioLegend) and human CD4, human CD8, and the GPC3-CAR as described above. IL15 and IL21 in blood plasma were measured using the MILLIPLEX MAP human cytokine/chemokine magnetic bead kit (EMD Millipore).

To measure the ability of inducible Caspase 9 (iC9) to eliminate IL15 and IL21 producing cells, the construct iC9.21.15.NGFR was generated by infusion cloning. In brief, the fragment of IL21 and IL15 was amplified from 21.15.GBBz and fused in frame with the amplicons of iC9 (33) and the truncated Neural Growth Factor Receptor (NGFR)(34). T cells were co-transduced with GBBz, iC9.21.15.NGFR and Ffluc to track their *in vivo* expansion and persistence with bioluminescence imaging. The chemical inducer of dimerization AP20187 (Clontech Laboratories; Cat #: 635069) was dissolved according to the manufacturers instructions given at 50 μ g/mouse dose ip in 100 μ l solution on Days 8 and 10 post-adoptive transfer.

Statistical analyses

Data were summarized using descriptive statistics. One-way or two-way ANOVAs adjusted for donor effect followed if applicable by pairwise comparisons between groups were carried out. Response variables were log-transformed, if necessary, to achieve normality. Analysis was performed using SAS version 9.4. P values < 0.05 were considered statistically significant

Results:

T cells effectively co-expressed IL21 and/or IL15 with a GPC3-CAR from a single retroviral construct.

We generated a set of CAR constructs based on our previously optimized GBBz GPC3-CAR (27) with additional sequence(s) for human IL21 and/or IL15 (Fig. 1A) using the clinically validated Moloney murine leukemia virus-derived SFG retroviral vector backbone. After transduction, all constructs were stably expressed by human peripheral blood T cells, with

constructs containing IL21 (21.GBBz and 21.15.GBBz) demonstrating slightly lower overall transduction efficiency compared to the GBBz construct ($p < 0.001$; Fig. 1B).

To measure IL15 and IL21 production, supernatants were collected from GPC3-CAR T cells cultured with and without GPC3-positive tumor cells and evaluated by ELISA. IL15 and IL21 were indeed secreted by CAR T cells engineered to express the corresponding genes at baseline (Fig. 1C and D). Following CAR stimulation by GPC3-positive HCC cells, IL15 and IL21 production increased significantly from T cells co-expressing the corresponding transgenes ($p < 0.001$), and IL21 concentrations remained significantly higher than IL15 ($p < 0.001$). Whereas T cells expressing 15.GBBz produced significantly more IL15 than 21.15.GBBz T cells at baseline ($p < 0.01$) and after stimulation ($p < 0.001$), IL21 production did not differ between 21.GBBz and 21.15.GBBz groups in either condition. Given that IL15 and/or IL21 could potentially induce antigen-independent T cell proliferation, we evaluated the ability of each T cell group to maintain autonomous growth. Whereas all groups underwent an initial burst of proliferation after transduction, in the absence of antigen stimulation, no viable CAR T cells remained in any group after 50 days (Supplemental Fig. S1).

In summary, transduced T cells stably expressed GPC3-CAR constructs and produced significant quantities of one or both cytokines, as appropriate, without evidence of antigen-independent autonomous growth.

IL15 and/or IL21 co-expression altered the effector cytokine production profile of GPC3-CAR T cells

We next explored whether IL21 and/or IL15 co-expression impacts the efficacy and/or specificity of GPC3-CAR-mediated tumor cell killing using a chromium-51 release assay (27). T cells expressing any of the four GPC3-CAR constructs specifically and effectively lysed GPC3-positive tumor cells (Huh-7, Hep3B, G401, A549-GPC3) in an antigen-dependent manner regardless of IL-21/IL15 co-expression (Fig. 2A).

To evaluate an additional measure of T cell activation, we determined the T_H1 and T_H2 effector cytokine production profiles of GPC3-CAR T cells following co-culture with GPC3-positive or -negative target cells. GPC3-negative A549 cells did not induce significant effector cytokine production suggesting that the GPC3-CARs in this study do not trigger consequential tonic signaling (Supplemental Fig. S2). CAR engagement by GPC3-positive Huh-7 cells specifically induced cytokine production by GPC3-CAR T cells but not by control groups (Fig. 2B and Supplemental Fig. S2). IL15 co-expression caused a significant decrease in IL-13 production compared to T cells expressing constructs without IL15 ($p < 0.001$; Fig. 2B). A similar decline was observed for GM-CSF in 15.GBBz but not in 21.15.GBBz T cells ($p = 0.0052$). IL21 co-expression significantly enhanced IL-2 production compared to groups lacking IL21 (21.15.GBBz vs GBBz, $p = 0.0047$; 21.GBBz vs GBBz, $p = 0.0016$).

Cytokine release syndrome (CRS) and neurotoxicity are serious and potentially lethal side effects of CAR T cell therapies and are primarily mediated by IL-1 and IL-6 produced by monocyte/macrophages (35). These myeloid cells can be influenced by TNF α , IFN- γ and

GM-CSF which are predictors of severe CRS (36). In co-culture systems, we detected no difference in IL1 and IL6 produced by monocyte/macrophages cells between GPC3-CAR T cell groups suggesting that the co-expression of IL15 or IL21 was unlikely to increase the risk of CRS or neurotoxicity (Supplemental Fig. S3).

CD4⁺ and CD8⁺ T cells can produce different effector cytokines (37) and CD8⁺ T cell homeostasis is supported by IL15 which is expressed in 15.GBBz and 21.15.GBBz T cells. To examine if the differences in effector cytokine production were related to differences in CD4/CD8 composition, we evaluated this parameter at baseline and following tumor cell engagement (Fig. 2C). We found that combined expression of IL15 and IL21 increased the CD8⁺ GPC3-CAR T cell population (with a corresponding decrease in the CD4 population) versus GBBz alone at baseline (p=0.0436). Following two rounds of stimulation, the CD8⁺ subset was enriched in 15.GBBz and 21.15.GBBz T cell groups (p=0.0478 and p=0.0078, respectively; Fig. 2C and Supplemental Fig. S4A).

Overall, GPC3-CAR T cells demonstrated effective GPC3-specific short-term cytotoxic activity *in vitro* regardless of cytokine co-expression. The cells underwent IL15 and/or IL-21-specific changes in both cytokine production profile and CD4/CD8 T cell phenotype distribution that could have benefitted their antitumor efficacy.

Combined expression of IL15 and IL21 increased the proportion of less differentiated GPC3-CAR T cells

Limited *in vivo* expansion is a major barrier for effective immunotherapy against solid tumors. To test the proliferative capacity of GPC3-CAR T cells, we repeatedly exposed them to fresh tumor cells *in vitro* every 3–4 days in the absence of exogenous cytokines. After the second round of stimulation with fresh HCC cells (day 7), T cells expressing GBBz, 15.GBBz, and 21.15.GBBz began to expand to higher numbers than 21.GBBz T cells and control groups (21.15.GBBz/15.GBBz vs 21.GBBz, p<0.001; GBBz vs 21.GBBz, p=0.0486, Fig. 3A). By the end of the third stimulation (day 10), 21.15.GBBz and 15.GBBz T cells expanded significantly more than the GBBz group (15.GBBz vs. GBBz, p=0.0013; 21.15.GBBz vs. 15.GBBz, p=0.0243), suggesting a critical role for IL15 in enhancing expansion. After the fourth stimulation (day 14), only 21.15.GBBz T cells continued to proliferate, yielding significantly higher cell numbers than all other groups (p<0.001).

To explore which factors may have contributed to the increased proliferative capacity of 21.15.GBBz T cells, we measured the subset composition among the four CAR T cell groups. Compared to GBBz T cells, both 21.GBBz and 21.15.GBBz T cells displayed a significantly higher proportion of CD4⁺ central memory cells (T_{cm}, CD45RO⁺/CD62L⁺; p=0.0035 and p<0.001, respectively) and of CD8⁺ stem cell memory / naïve cells (T_{scm/Tn}, CD45RO⁻/CD62L⁺; p=0.014 and p=0.012, respectively; Fig. 3B). After stimulation with tumor cells, these differences were no longer detected (Supplemental Fig. S4B and C). Although CD8⁺ 21.GBBz T cells had a higher proportion of less differentiated cells, these cells also expressed higher amounts of TIM-3 (p=0.0012) at baseline and significantly higher expression of LAG-3, TIM-3, and PD-1 (p<0.001, p=0.001, and p=0.0138, respectively) after stimulation with HCC compared to GBBz cells, indicating an exhausted phenotype (Fig. Supplemental Fig. S5).

Next, we examined whether the observed differences in proliferation were related to differences in rates of apoptosis using annexin-V staining. We found that co-expression of IL15 alone or in combination with IL21 decreased the rate of apoptosis in T cells resulting in more live cells compared with GBBz alone following three rounds of stimulation with GPC3-positive tumor cells ($p=0.0015$, as measured on day 9; Fig. 3C). This finding corresponded to the superior expansion of 21.15.GBBz T cells observed in Fig. 3A. Thus, the superior *in vitro* expansion of GPC3-CAR T cells co-expressing IL15 and IL21 was associated with a lower apoptosis rate and increased T_{scm}/T_n and T_{cm} populations.

IL21 and IL15 co-expression maintained TCF-1 expression in GPC3-CAR T cells.

To explore the mechanisms driving differences in proliferation between GPC3-CAR T cell groups, we examined gene expression profiles before and after exposure to GPC3-positive HCC cells. We detected significant differences in overall expression patterns at baseline (after manufacturing) in 21.GBBz and 21.15.GBBz T cells compared to GBBz T cells (day 0; Supplemental Fig. S6A-C and Supplemental Fig. S7). Following stimulation with HCC cells (day 3), the gene expression profiles of 15.GBBz, 21.GBBz and 21.15.GBBz T cells were different from that of GBBz T cells (Fig. 4A and Supplemental Fig. S6D-F) with global differences included genes related to cytotoxicity (*GZMA*, *GZMB*, *PRFI*), chemotaxis (*CCR1*, *CCR2*, *CCR5*), and apoptosis/survival (*BCL-2*, *TCF7/TCF-1*).

Since IL15 and IL21 co-expressing CAR T cells had improved proliferation/survival, we focused on genes related to apoptosis and proliferation and found that *BCL-2* and *TCF7* were overexpressed in 15.GBBz and 21.15.GBBz compared to GBBz T cells ($p=0.023$ and 0.0025 , respectively; Supplemental Fig. S6D-F). No difference was detected at the protein level for BCL-2 (Supplemental Fig. S8), suggesting that it does not play a key role in the enhanced survival of 21.15.GBBz T cells. The TCF-1 protein, encoded by *TCF7*, is a critical transcription factor for T cell development, expansion, and survival (38,39). Prior to stimulation (day 0), the *TCF7* gene was expressed similarly in all the GPC3-CAR T cell groups (Supplemental Fig. S6A-C). After stimulation with HCC cells, the gene expression of *TCF7* was significantly increased in 21.GBBz (2.2-fold increase, $p=0.014$), 15.GBBz (2.3-fold increase, $p=0.028$), and to an even greater extent in 21.15.GBBz T cells (4.1-fold increase, $p=0.0003$) compared to in GBBz T cells (Fig. 4A). The proportion of TCF-1 (protein)-positive cells at baseline was significantly higher in 21.15.GBBz T cells compared to other CAR T cell groups (21.15.GBBz vs 15.GBBz in CD4 subset: $p=0.0223$; in CD8 subset: $p<0.001$, Fig. 4B and C). The expression of either IL-15, IL21, or the combination improved TCF-1 protein expression in both CD4⁺ and CD8⁺ CAR T cells (Fig. 4B and C). After two consecutive stimulations with tumor cells, the percent of TCF-1-positive cells was the highest in 21.15.GBBz T cell group for the CD4 subset (21.GBBz vs 21.15.GBBz, $p=0.002$; 15.GBBz vs 21.15.GBBz, $p=0.0296$) whereas in the CD8 subset, the 15.GBBz and 21.15.GBBz T cells had the highest percentage of TCF-1-positive cells (15.GBBz vs 21.GBBz $p=0.0124$; 21.GBBz vs 21.15.GBBz $p<0.001$; Fig. 4C). TCF-1 expression in the CD8 subset remained highest after two stimulations in the 21.15.GBBz group compared to all other groups (21.GBBz vs 21.15.GBBz, $p=0.0044$, Fig. 4D).

To determine whether TCF-1 was required for the enhanced proliferative capacity of 21.15.GBBz T cells, we knocked out *TCF7* with CRISPR-Cas9 and measured CAR T cell expansion upon repeated engagement with GPC3-positive tumor cells (Supplemental Fig. S9). We found that *TCF7*-KO eliminated the proliferative benefit of 21.15.GBBz T cells compared to GBBz T cells (Fig. 4E). These results suggested that IL21 and IL15 mediated maintenance of TCF-1-positive cells was responsible for the increased proliferative capacity of 21.15.GBBz T cells.

Co-expression of IL15 and IL21 enhanced *in vivo* expansion, persistence, and antitumor activity of GPC3-CAR T cells.

To evaluate the *in vivo* expansion and persistence of GPC3-CAR T cells, we established HCC xenografts in NSG mice and injected T cells co-transduced with the individual GPC3-CAR constructs and an eGFP.Ffluc construct optimized for tracking small numbers of cells *in vivo* via bioluminescence imaging (Fig. 5A)(32). As observed in our previous study (27), GBBz T cells expanded effectively for eight days, after which the population contracted and disappeared entirely by 15 days post-injection (Fig. 5B and C)(27). 21.GBBz and 15.GBBz T cells had a similar timeline of peak expansion compared to GBBz T cells but persisted longer *in vivo* before their numbers began to decline (day 12, $p < 0.001$). Co-expression of IL15 and IL21 induced the highest expansion and sustained persistence of GPC3-CAR T cells *in vivo* (day 15, 21.15.GBBz vs 21.GBBz $p = 0.0012$). Peripheral blood analysis 15 days after adoptive transfer showed increased frequency of CD8⁺ 15.GBBz and 21.15.GBBz T cells compared to GBBz T cells ($p = 0.0076$ and $p < 0.0002$, respectively; Supplemental Fig. S10). In the spleen, the frequency of CD4⁺ 21.GBBz and 21.15.GBBz CAR T cells was significantly elevated compared to GBBz T cells ($p = 0.0386$ and $p = 0.003$, respectively). The frequency of CD8⁺ 21.15.GBBz cells was significantly higher in the spleen compared to other groups including 15.GBBz ($p = 0.0083$; Fig. 5D).

As a safety assessment, serum concentrations of IL15 and IL21 were measured in all therapeutic groups (day 15). IL21 and IL15 serum concentrations in mice treated with cytokine-containing CAR T cells were similar to those of control and GBBz T cell-infused mice at the peak of expansion (Supplemental Fig. S11A and B). As an additional safety measure, we evaluated if the co-expression of the clinically validated inducible Caspase 9 (iC9) could prevent the proliferation of 21.15.GBBz T cells *in vivo*. We found that after administering AP20187, the chemical inducer of dimerization intravenously, 21.15.GBBz can be effectively eliminated in tumor bearing mice. Thus, iC9 suicide switch may be used, if necessary, in the clinical setting for unexpected toxicities (Supplemental Fig. S11C-E).

Finally, to evaluate the effects of IL15 and IL21 co-expression on the antitumor activity of GPC3-CAR T cells, we adoptively transferred these cells into mice bearing *Ffluc*-labeled tumor xenografts and monitored tumor growth weekly. In a relatively slow-growing GPC3⁺ malignant rhabdoid tumor model, co-expression of IL15 and/or IL21 significantly enhanced the antitumor responses after injection of GPC3-CAR T cells (week 5: 21.15.GBBz / 15.GBBz vs GBBz, $p < 0.001$; 21.GBBz vs GBBz, $p = 0.0011$, Supplemental Fig. S12), and IL15 co-expressing CAR T cell groups induced a more rapid antitumor effect (week 5: 21.15.GBBz / 15.GBBz vs 21.GBBz, $p < 0.001$). Next, we examined GPC3-CAR T cell

antitumor responses in a rapidly growing HCC xenograft model injecting 2×10^6 CAR T cells. We found that 15.GBBz and 21.15.GBBz T cells mediated superior antitumor activity compared to GBBz or 21.GBBz T cells and control groups ($p < 0.001$; Supplemental Fig. S13). In this model, 21.15.GBBz T cells eliminated tumors more rapidly than 15.GBBz T cells (week 4, $p < 0.001$). Lastly, to further stress the antitumor potential of GPC3-CAR T cells, we injected a low dose of 5×10^5 CAR T cells in mice engrafted with rapidly growing HCC xenografts. At this dose, only 21.15.GBBz T cells, but not 15.GBBz T cells, maintained antitumor activity, which translated into significant survival advantage (15.GBBz vs 21.15.GBBz, $p < 0.001$, Fig. 5E-G). These results demonstrated that 21.15.GBBz T cells had superior expansion, persistence and antitumor activity against HCC *in vivo*.

Discussion:

Here, we showed preclinical evidence that human GPC3-CAR T cells co-expressing IL15 and IL21 had superior expansion and antitumor activity in preclinical models of HCC. Gene expression analysis identified TCF-1 as a key transcription factor associated with the increased proliferative capacity of 21.15.GBBz T cells.

We found that co-expression of IL21 and/or IL15 with GBBz did not impact the potent, specific, short-term *in vitro* cytolytic activity of T cells against HCC tumors cells; in contrast, we did detect significant differences in effector cytokine production polarization when comparing GBBz T cells to those co-expressing one or both cytokines. As in our previous study, GBBz T cells secreted a T_H1 -polarized cytokine profile (high IFN- γ and GM-CSF; low IL10 and IL4)(27). This overall trend was recapitulated in the current study, with CAR T cell groups showing GBBz-mediated T_H1 polarization regardless of cytokine co-expression. However, we found a striking decrease in IL13 production in CAR T cells co-expressing IL15 (15.GBBz and 21.15.GBBz T cells). IL13 is a T_H2 -cytokine primarily produced by $CD4^+$ T cells that generates many of the same biological effects as IL4, including decreasing the antitumor function of T cells and promoting tumor cell proliferation (40,41). IL13 also plays an important role in homeostasis of myeloid-derived suppressor cells (MDSCs), which can dampen the efficacy of immunotherapies, increase metastasis formation, cancer progression and inhibit CAR T cell activity(41–45); therefore, limiting the amount of IL13 in the tumor microenvironment may enhance the therapeutic potential of CAR T cells (45,46).

Since expansion and persistence of CAR T cells are strong predictors of clinical activity, a key objective of this study was to improve these parameters. We demonstrated that co-expression of IL15 and IL21 in GPC3-CAR T cells increased the proportion of naive/stem cell memory and central memory GPC3-CAR T cells post-manufacture. These less-differentiated T cells have greater proliferative capacity than more mature cells (47–49), providing a potential proliferative advantage for GPC3-CAR T cells co-expressing IL21. Given that all experimental groups were manufactured under the same culture conditions including supplementation with IL15 and IL21, this finding was unexpected. Continuous production of IL21 via transgenic expression from the GPC3-CAR throughout the culturing process likely influenced the T cell phenotype.

We determined that compared to other experimental groups, co-expression of IL15 alone or in combination with IL21 decreased the proportion of transduced T cells undergoing apoptosis after multiple stimulations with HCC tumor cells; thus, proportionately increasing surviving CAR T cells. Finally, we found that the *TCF7* gene encoding TCF-1, a key transcription factor in T cell development, expansion, memory formation, and survival (38,39,50,51), was more highly expressed in the CD8⁺ subsets of GPC3-CAR T cells expressing IL15, IL21, or both compared to in CD8⁺ GBBz T cells. Following two rounds of stimulation with HCC cells, TCF-1 expression was highly maintained in 21.15.GBBz T cells and was associated with enrichment for and continued expansion of CD8⁺ CAR T cells. CRISPR-Cas9 knock-out of *TCF7* eliminated the proliferative advantage of 21.15.GBBz T cells suggesting that TCF-1 plays a role in enhancing the expansion and survival of IL-15- and IL-21-co-expressing GPC3-CAR T cells.

In cancer patients, the effector to target ratio of CAR T cells to cancer cells greatly favors cancer; thus, its complete elimination requires CAR T cells to kill repeatedly and expand. In sequential killing assays, in which GPC3-CAR T cells are repeatedly exposed to fresh tumor cells in vitro, we found that combined expression of IL15 and IL21 resulted in the most expansion. Additionally, in an aggressive xenograft model of HCC treated with the lowest dose of GPC3-CAR T cells, thereby stressing their functional capacity, cells transduced with 21.15.GBBz resulted in significant survival advantage. These findings suggest that IL15 and IL21 should provide the most potent antitumor activity in the clinical setting.

Safety remains a central requirement for all cancer treatments. Elevated concentrations of IL15 and IL21 can cause side effects as described in early phase studies of subcutaneous or intravenous recombinant IL21 and IL15 administration in patients with cancer (52). In these studies, at the maximum tolerated dose (MTD), peripheral blood peak concentrations of IL15 and IL21 were 1608 pg/ml and 141 ng/ml, respectively (53,54). In mice infused with GPC3-CAR T cells expressing IL15 and/or IL21, cytokine concentrations at the peak of T cell expansion remained 100–1000-fold below the peak corresponding MTDs measured in humans. Therefore, we do not anticipate systemic toxicities in patients treated with GPC3-CAR T cells co-expressing IL15 and/or IL21. Nevertheless, we show that the use of inducible Caspase 9 can effectively eliminate IL15 and IL21 expressing GPC3-CAR T cells in vivo; thus, this “suicide switch” system may be used during clinical evaluation(33).

In conclusion, GPC3-CAR T cells co-expressing IL15 and IL21 were effective at treating HCC in preclinical models. Our findings address a major barrier by enhancing the expansion and persistence of therapeutic cells, resulting robust antitumor responses. We provided mechanistic insight and preclinical evidence to substantiate testing GPC3-CAR T cells co-expressing IL15 and IL21 in patients, an avenue that will be explored in two ongoing clinical trials ([NCT02932956](#); [NCT02905188](#)).

Supplementary Material

Refer to Web version on PubMed Central for supplementary material.

Acknowledgement:

We thank Dr. Malcolm Brenner (Center for Cell and Gene Therapy, BCM, Houston, TX) for helpful discussions. We also thank Elise Shen for help in animal experiments, Erica Di Piero (Texas Children's Cancer Center, Department of Pediatrics, Baylor College of Medicine, Houston, TX) and Catherine Gillespie (Center for Cell and Gene Therapy, Baylor College of Medicine, Houston, TX) for helpful edits of this manuscript.

Financial support:

National Institute of Health S10 OD020066 to the Texas Children's Flow Cytometry Core. American Cancer Society Mentored Scholar Award for AH.

References:

1. Villanueva A. Hepatocellular Carcinoma. *N Engl J Med* 2019;380(15):1450–62 doi 10.1056/NEJMra1713263. [PubMed: 30970190]
2. Maude SL, Frey N, Shaw PA, Aplenc R, Barrett DM, Bunin NJ, et al. Chimeric antigen receptor T cells for sustained remissions in leukemia. *N Engl J Med* 2014;371(16):1507–17 doi 10.1056/NEJMoa1407222. [PubMed: 25317870]
3. Davila ML, Riviere I, Wang X, Bartido S, Park J, Curran K, et al. Efficacy and toxicity management of 19–28z CAR T cell therapy in B cell acute lymphoblastic leukemia. *Sci Transl Med* 2014;6(224):224ra25 doi 10.1126/scitranslmed.3008226.
4. Turtle CJ, Hanafi LA, Berger C, Gooley TA, Cherian S, Hudecek M, et al. CD19 CAR-T cells of defined CD4+:CD8+ composition in adult B cell ALL patients. *J Clin Invest* 2016;126(6):2123–38 doi 10.1172/JCI85309. [PubMed: 27111235]
5. Turtle CJ, Hanafi LA, Berger C, Hudecek M, Pender B, Robinson E, et al. Immunotherapy of non-Hodgkin's lymphoma with a defined ratio of CD8+ and CD4+ CD19-specific chimeric antigen receptor-modified T cells. *Sci Transl Med* 2016;8(355):355ra116 doi 10.1126/scitranslmed.aaf8621.
6. Lee DW, Kochenderfer JN, Stetler-Stevenson M, Cui YK, Delbrook C, Feldman SA, et al. T cells expressing CD19 chimeric antigen receptors for acute lymphoblastic leukaemia in children and young adults: a phase 1 dose-escalation trial. *Lancet* 2015;385(9967):517–28 doi 10.1016/S0140-6736(14)61403-3. [PubMed: 25319501]
7. Bo Zhai DS, Gao Huiping, Qi Xingxing, Jiang Hua, Zhang Yuan, Chi Jiachang, Ruan Huaying, Wang Huamao, Qinhuo Cindy Ru Zonghai Li. A phase I study of anti-GPC3 chimeric antigen receptor modified T cells (GPC3 CAR-T) in Chinese patients with refractory or relapsed GPC3+ hepatocellular carcinoma (r/r GPC3+ HCC). *J Clin Oncol* 2017;35(2017 (suppl; abstr 3049)).
8. Heczey A, Louis CU, Savoldo B, Dakhova O, Durett A, Grilley B, et al. CAR T Cells Administered in Combination with Lymphodepletion and PD-1 Inhibition to Patients with Neuroblastoma. *Molecular therapy : the journal of the American Society of Gene Therapy* 2017;25(9):2214–24 doi 10.1016/j.ymthe.2017.05.012. [PubMed: 28602436]
9. Ahmed N, Brawley V, Hegde M, Bielamowicz K, Kalra M, Landi D, et al. HER2-Specific Chimeric Antigen Receptor-Modified Virus-Specific T Cells for Progressive Glioblastoma: A Phase 1 Dose-Escalation Trial. *JAMA Oncol* 2017 doi 10.1001/jamaoncol.2017.0184.
10. Ahmed N, Brawley VS, Hegde M, Robertson C, Ghazi A, Gerken C, et al. Human Epidermal Growth Factor Receptor 2 (HER2) -Specific Chimeric Antigen Receptor-Modified T Cells for the Immunotherapy of HER2-Positive Sarcoma. *J Clin Oncol* 2015;33(15):1688–96 doi 10.1200/JCO.2014.58.0225. [PubMed: 25800760]
11. Park JR, Digiusto DL, Slovak M, Wright C, Naranjo A, Wagner J, et al. Adoptive transfer of chimeric antigen receptor re-directed cytolytic T lymphocyte clones in patients with neuroblastoma. *Molecular therapy : the journal of the American Society of Gene Therapy* 2007;15(4):825–33 doi 10.1038/sj.mt.6300104. [PubMed: 17299405]
12. Louis CU, Savoldo B, Dotti G, Pule M, Yvon E, Myers GD, et al. Antitumor activity and long-term fate of chimeric antigen receptor-positive T cells in patients with neuroblastoma. *Blood* 2011;118(23):6050–6 doi 10.1182/blood-2011-05-354449. [PubMed: 21984804]

13. Pilipow K, Roberto A, Roederer M, Waldmann TA, Mavilio D, Lugli E. IL15 and T-cell Stemness in T-cell-Based Cancer Immunotherapy. *Cancer Res* 2015;75(24):5187–93 doi 10.1158/0008-5472.Can-15-1498. [PubMed: 26627006]
14. Davis MR, Zhu Z, Hansen DM, Bai Q, Fang Y. The role of IL-21 in immunity and cancer. *Cancer Lett* 2015;358(2):107–14 doi 10.1016/j.canlet.2014.12.047. [PubMed: 25575696]
15. Hoyos V, Savoldo B, Quintarelli C, Mahendravada A, Zhang M, Vera J, et al. Engineering CD19-specific T lymphocytes with interleukin-15 and a suicide gene to enhance their anti-lymphoma/leukemia effects and safety. *Leukemia* 2010;24(6):1160. [PubMed: 20428207]
16. Markley JC, Sadelain M. IL-7 and IL-21 are superior to IL-2 and IL-15 in promoting human T cell–mediated rejection of systemic lymphoma in immunodeficient mice. *Blood* 2010;115(17):3508–19. [PubMed: 20190192]
17. Krenciute G, Prinzing BL, Yi Z, Wu MF, Liu H, Dotti G, et al. Transgenic Expression of IL15 Improves Antiglioma Activity of IL13Ralpha2-CAR T Cells but Results in Antigen Loss Variants. *Cancer Immunol Res* 2017;5(7):571–81 doi 10.1158/2326-6066.CIR-16-0376. [PubMed: 28550091]
18. Chen Y, Sun C, Landoni E, Metelitsa LS, Dotti G, Savoldo B. Eradication of neuroblastoma by T cells redirected with an optimized GD2-specific chimeric antigen receptor and interleukin-15. *Clinical cancer research : an official journal of the American Association for Cancer Research* 2019 doi 10.1158/1078-0432.Ccr-18-1811.
19. Strengell M, Matikainen S, Siren J, Lehtonen A, Foster D, Julkunen I, et al. IL-21 in synergy with IL-15 or IL-18 enhances IFN-gamma production in human NK and T cells. *J Immunol* 2003;170(11):5464–9. [PubMed: 12759422]
20. Zeng R, Spolski R, Finkelstein SE, Oh S, Kovanan PE, Hinrichs CS, et al. Synergy of IL-21 and IL-15 in regulating CD8+ T cell expansion and function. *J Exp Med* 2005;201(1):139–48 doi 10.1084/jem.20041057. [PubMed: 15630141]
21. Chan ES, Pawel BR, Corao DA, Venneti S, Russo P, Santi M, et al. Immunohistochemical expression of glypican-3 in pediatric tumors: an analysis of 414 cases. *Pediatr Dev Pathol* 2013;16(4):272–7 doi 10.2350/12-06-1216-OA.1. [PubMed: 23530909]
22. Toretsky JA, Zitomersky NL, Eskenazi AE, Voigt RW, Strauch ED, Sun CC, et al. Glypican-3 expression in Wilms tumor and hepatoblastoma. *J Pediatr Hematol Oncol* 2001;23(8):496–9. [PubMed: 11878776]
23. Yamauchi N, Watanabe A, Hishinuma M, Ki Ohashi, Midorikawa Y, Morishita Y, et al. The glypican 3 oncofetal protein is a promising diagnostic marker for hepatocellular carcinoma. *Mod Pathol* 2005;18(12):1591–8. [PubMed: 15920546]
24. Haruyama Y, Kataoka H. Glypican-3 is a prognostic factor and an immunotherapeutic target in hepatocellular carcinoma. *World J Gastroenterol* 2016;22(1):275–83 doi 10.3748/wjg.v22.i1.275. [PubMed: 26755876]
25. Kinoshita Y, Tanaka S, Souzaki R, Miyoshi K, Kohashi K, Oda Y, et al. Glypican 3 expression in pediatric malignant solid tumors. *Eur J Pediatr Surg* 2015;25(1):138–44 doi 10.1055/s-0034-1393961. [PubMed: 25344940]
26. Gao H, Li K, Tu H, Pan X, Jiang H, Shi B, et al. Development of T cells redirected to glypican-3 for the treatment of hepatocellular carcinoma. *Clinical cancer research : an official journal of the American Association for Cancer Research* 2014;20(24):6418–28 doi 10.1158/1078-0432.CCR-14-1170. [PubMed: 25320357]
27. Li W, Guo L, Rathi P, Marinova E, Gao X, Wu MF, et al. Redirecting T Cells to Glypican-3 with 4–1BB Zeta Chimeric Antigen Receptors Results in Th1 Polarization and Potent Antitumor Activity. *Human gene therapy* 2017;28(5):437–48 doi 10.1089/hum.2016.025. [PubMed: 27530312]
28. Iwahori K, Kakarla S, Velasquez MP, Yu F, Yi Z, Gerken C, et al. Engager T cells: a new class of antigen-specific T cells that redirect bystander T cells. *Molecular therapy : the journal of the American Society of Gene Therapy* 2015;23(1):171–8 doi 10.1038/mt.2014.156. [PubMed: 25142939]
29. Ramos CA, Rouce R, Robertson CS, Reyna A, Narala N, Vyas G, et al. In Vivo Fate and Activity of Second- versus Third-Generation CD19-Specific CAR-T Cells in B Cell Non-

- Hodgkin's Lymphomas. *Molecular therapy : the journal of the American Society of Gene Therapy* 2018;26(12):2727–37 doi 10.1016/j.ymthe.2018.09.009. [PubMed: 30309819]
30. Pule MA, Straathof KC, Dotti G, Heslop HE, Rooney CM, Brenner MK. A chimeric T cell antigen receptor that augments cytokine release and supports clonal expansion of primary human T cells. *Mol Ther* 2005;12(5):933–41 doi S1525–0016(05)00186–3 [pii];10.1016/j.ymthe.2005.04.016 [doi].
 31. Gomes-Silva D, Srinivasan M, Sharma S, Lee CM, Davis TH, Rouse RH, et al. CD7-edited T cells expressing a CD7-specific CAR for the therapy of T-cell malignancies. *Blood* 2017 doi 10.1182/blood-2017-01-761320.
 32. Rabinovich BA, Ye Y, Etto T, Chen JQ, Levitsky HI, Overwijk WW, et al. Visualizing fewer than 10 mouse T cells with an enhanced firefly luciferase in immunocompetent mouse models of cancer. *Proc Natl Acad Sci U S A* 2008;105(38):14342–6 doi 10.1073/pnas.0804105105. [PubMed: 18794521]
 33. Di Stasi A, Tey SK, Dotti G, Fujita Y, Kennedy-Nasser A, Martinez C, et al. Inducible apoptosis as a safety switch for adoptive cell therapy. *N Engl J Med* 2011;365(18):1673–83 doi 10.1056/NEJMoa1106152. [PubMed: 22047558]
 34. Increased Transduction Efficiency of Primary Hematopoietic Cells by Physical Colocalization of Retrovirus and Target Cells. *Journal of Hematotherapy* 1998;7(3):217–24 doi 10.1089/scd.1.1998.7.217. [PubMed: 9621255]
 35. Norelli M, Camisa B, Barbiera G, Falcone L, Purevdorj A, Genua M, et al. Monocyte-derived IL-1 and IL-6 are differentially required for cytokine-release syndrome and neurotoxicity due to CAR T cells. *Nature medicine* 2018;24(6):739–48 doi 10.1038/s41591-018-0036-4.
 36. Teachey DT, Lacey SF, Shaw PA, Melnhorst JJ, Maude SL, Frey N, et al. Identification of Predictive Biomarkers for Cytokine Release Syndrome after Chimeric Antigen Receptor T-cell Therapy for Acute Lymphoblastic Leukemia. *Cancer discovery* 2016;6(6):664–79 doi 10.1158/2159-8290.Cd-16-0040. [PubMed: 27076371]
 37. *Janeway's Immunobiology. Ninth Edition* by Kenneth Murphy, Casey Weaver, Allan Mowat, Leslie Berg, David Chaplin, Charles A. Janeway, Paul Travers, and Mark Walport. *The Quarterly Review of Biology* 2018;93(1):59- doi 10.1086/696793.
 38. Weber BN, Chi AW, Chavez A, Yashiro-Ohtani Y, Yang Q, Shestova O, et al. A critical role for TCF-1 in T-lineage specification and differentiation. *Nature* 2011;476(7358):63–8 doi 10.1038/nature10279. [PubMed: 21814277]
 39. Kratchmarov R, Magun AM, Reiner SL. TCF1 expression marks self-renewing human CD8(+) T cells. *Blood advances* 2018;2(14):1685–90 doi 10.1182/bloodadvances.2018016279. [PubMed: 30021780]
 40. Park JM, Terabe M, Donaldson DD, Forni G, Berzofsky JA. Natural immunosurveillance against spontaneous, autochthonous breast cancers revealed and enhanced by blockade of IL-13-mediated negative regulation. *Cancer immunology, immunotherapy : CII* 2008;57(6):907–12 doi 10.1007/s00262-007-0414-0. [PubMed: 18004566]
 41. Terabe M, Park JM, Berzofsky JA. Role of IL-13 in regulation of anti-tumor immunity and tumor growth. *Cancer immunology, immunotherapy : CII* 2004;53(2):79–85 doi 10.1007/s00262-003-0445-0. [PubMed: 14610620]
 42. Kapanadze T, Gamrekelashvili J, Ma C, Chan C, Zhao F, Hewitt S, et al. Regulation of accumulation and function of myeloid derived suppressor cells in different murine models of hepatocellular carcinoma. *Journal of hepatology* 2013;59(5):1007–13 doi 10.1016/j.jhep.2013.06.010. [PubMed: 23796475]
 43. Yu SJ, Ma C, Heinrich B, Brown ZJ, Sandhu M, Zhang Q, et al. Targeting the crosstalk between cytokine-induced killer cells and myeloid-derived suppressor cells in hepatocellular carcinoma. *Journal of hepatology* 2019;70(3):449–57 doi 10.1016/j.jhep.2018.10.040. [PubMed: 30414862]
 44. Sinha P, Clements VK, Ostrand-Rosenberg S. Interleukin-13-regulated M2 Macrophages in Combination with Myeloid Suppressor Cells Block Immune Surveillance against Metastasis. *Cancer Research* 2005;65(24):11743–51 doi 10.1158/0008-5472.Can-05-0045. [PubMed: 16357187]

45. Long AH, Highfill SL, Cui Y, Smith JP, Walker AJ, Ramakrishna S, et al. Reduction of MDSCs with All-trans Retinoic Acid Improves CAR Therapy Efficacy for Sarcomas. *Cancer Immunol Res* 2016;4(10):869–80 doi 10.1158/2326-6066.Cir-15-0230. [PubMed: 27549124]
46. Parihar R, Rivas C, Huynh M, Omer B, Lapteva N, Metelitsa LS, et al. NK Cells Expressing a Chimeric Activating Receptor Eliminate MDSCs and Rescue Impaired CAR-T Cell Activity against Solid Tumors. *Cancer Immunol Res* 2019;7(3):363–75 doi 10.1158/2326-6066.Cir-18-0572. [PubMed: 30651290]
47. Terakura S, Yamamoto TN, Gardner RA, Turtle CJ, Jensen MC, Riddell SR. Generation of CD19-chimeric antigen receptor modified CD8+ T cells derived from virus-specific central memory T cells. *Blood* 2012;119(1):72–82 doi 10.1182/blood-2011-07-366419. [PubMed: 22031866]
48. Klebanoff CA, Gattinoni L, Torabi-Parizi P, Kerstann K, Cardones AR, Finkelstein SE, et al. Central memory self/tumor-reactive CD8+ T cells confer superior antitumor immunity compared with effector memory T cells. *Proc Natl Acad Sci U S A* 2005;102(27):9571–6 doi 10.1073/pnas.0503726102. [PubMed: 15980149]
49. Gattinoni L, Lugli E, Ji Y, Pos Z, Paulos CM, Quigley MF, et al. A human memory T cell subset with stem cell-like properties. *Nature medicine* 2011;17(10):1290–7 doi 10.1038/nm.2446.
50. Gautam S, Fioravanti J, Zhu W, Le Gall JB, Brohawn P, Lacey NE, et al. The transcription factor c-Myb regulates CD8(+) T cell stemness and antitumor immunity. *Nat Immunol* 2019;20(3):337–49 doi 10.1038/s41590-018-0311-z. [PubMed: 30778251]
51. Xing S, Li F, Zeng Z, Zhao Y, Yu S, Shan Q, et al. Tcf1 and Lef1 transcription factors establish CD8(+) T cell identity through intrinsic HDAC activity. *Nat Immunol* 2016;17(6):695–703 doi 10.1038/ni.3456. [PubMed: 27111144]
52. Spolski R, Leonard WJ. Interleukin-21: a double-edged sword with therapeutic potential. *Nat Rev Drug Discov* 2014;13(5):379–95 doi 10.1038/nrd4296. [PubMed: 24751819]
53. Thompson JA, Curti BD, Redman BG, Bhatia S, Weber JS, Agarwala SS, et al. Phase I study of recombinant interleukin-21 in patients with metastatic melanoma and renal cell carcinoma. *J Clin Oncol* 2008;26(12):2034–9 doi 10.1200/JCO.2007.14.5193. [PubMed: 18347008]
54. Conlon KC, Lugli E, Welles HC, Rosenberg SA, Fojo AT, Morris JC, et al. Redistribution, hyperproliferation, activation of natural killer cells and CD8 T cells, and cytokine production during first-in-human clinical trial of recombinant human interleukin-15 in patients with cancer. *J Clin Oncol* 2015;33(1):74–82 doi 10.1200/JCO.2014.57.3329. [PubMed: 25403209]

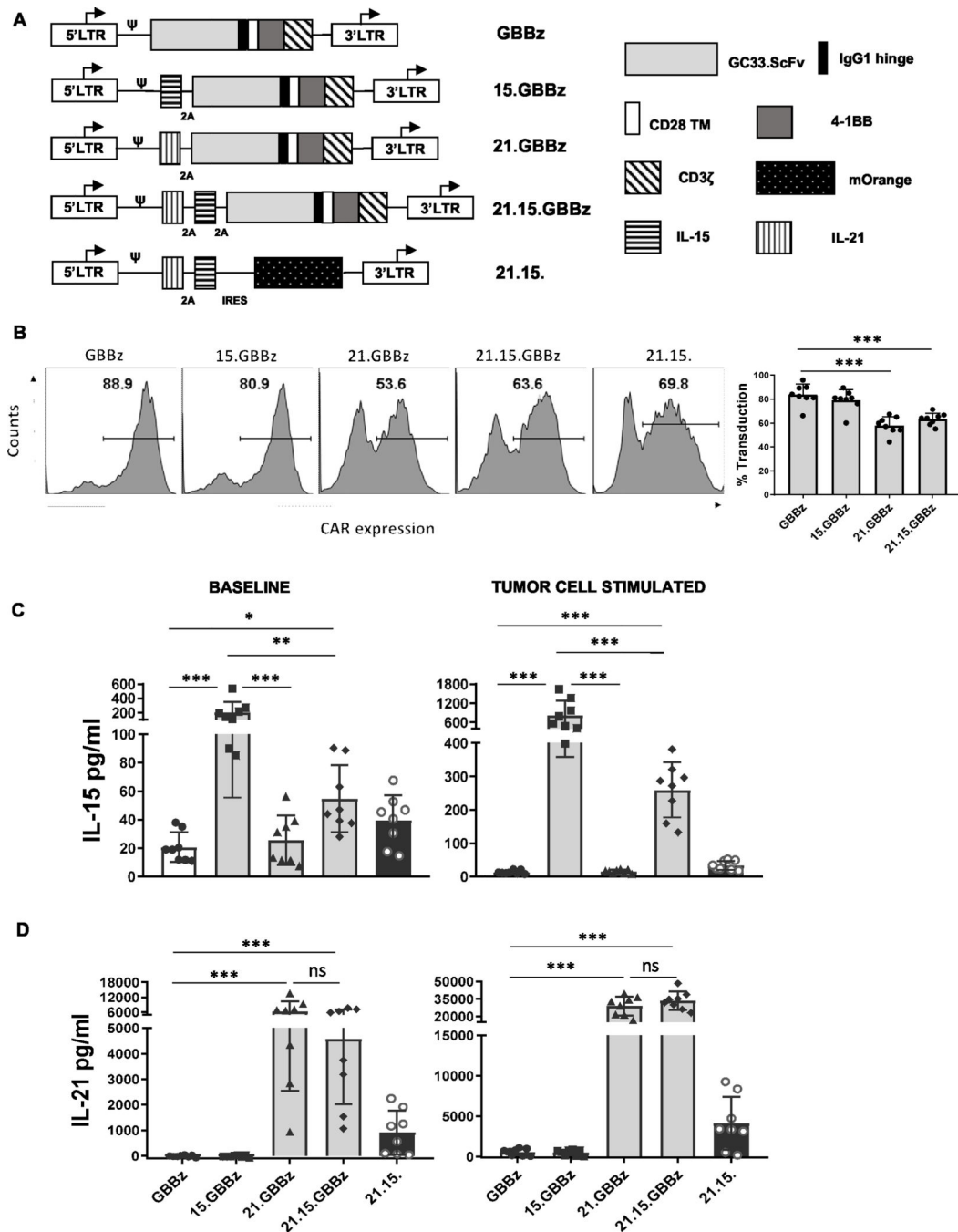


Figure 1. Generation of GPC3-CAR T cells that co-express IL21 and IL-15.

A) Schematic of retroviral constructs encoding GPC3-CAR (GBBz) with and without IL15 and/or IL-21. **B)** CAR expression in T cells transduced (on Day 3 post stimulation with plate bound antibody) using retroviral vectors containing the indicated GPC3-CAR constructs as measured by flow cytometry (on Days 10–14). Data from one representative donor and summary for eight independent donors in independent expansions is shown (mean \pm SD). IL15 (**C**) and IL21 (**D**) produced by the indicated T cell groups at baseline (left) or after

stimulation with GPC3-positive Huh-7 cells (right, E:T = 1:1, +72 hrs) as measured by ELISA (mean \pm SD, n=8). One-way ANOVA. * $p < 0.05$, ** $p < 0.01$, *** $p < 0.001$.

Author Manuscript

Author Manuscript

Author Manuscript

Author Manuscript

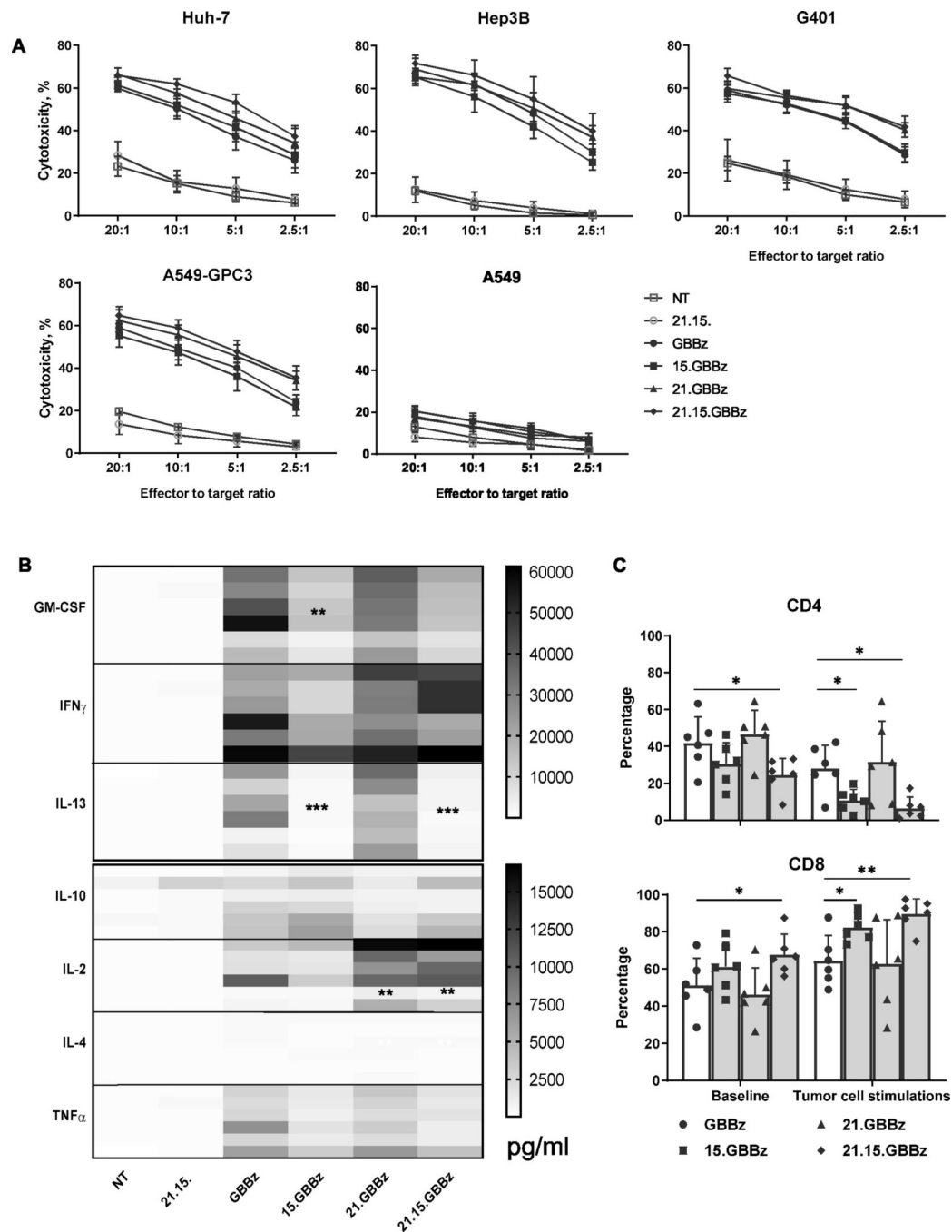


Figure 2. Co-expression of IL15 and/or IL21 maintained GPC3-specific tumor cell killing but altered effector cytokine release in GPC3-CAR T cells.

A) GPC3-CAR T cells were co-cultured with ^{51}Cr -labeled GPC3-positive (Huh-7, Hep3B, G401, A549-GPC3) and negative (A549) target cells at the indicated effector-to-target (E:T) ratios. ^{51}Cr -release was detected after four hours as a measure of GPC3-CAR T cytotoxicity (mean \pm SEM, pooled results from two independent experiments evaluating four donors). **B)** Indicated T cell groups were cultured with Huh-7 tumor cells at a 1:1 ratio and concentration of indicated effector cytokines released into the supernatant (+24

hrs) was measured by Luminex assay (combined data from three independent experiments evaluating six donors). Comparison with two-way ANOVA. C) Surface expression of CD4 (top) and CD8 (bottom) populations within CAR-positive cells at baseline (left) and after two consecutive stimulations with Huh-7 cells (right, E:T = 1:1) as measured by FACS (mean \pm SD, combined data from three independent experiments evaluating six donors), one-way ANOVA. *p<0.05, ** p<0.01, ***p<0.001.

Author Manuscript

Author Manuscript

Author Manuscript

Author Manuscript

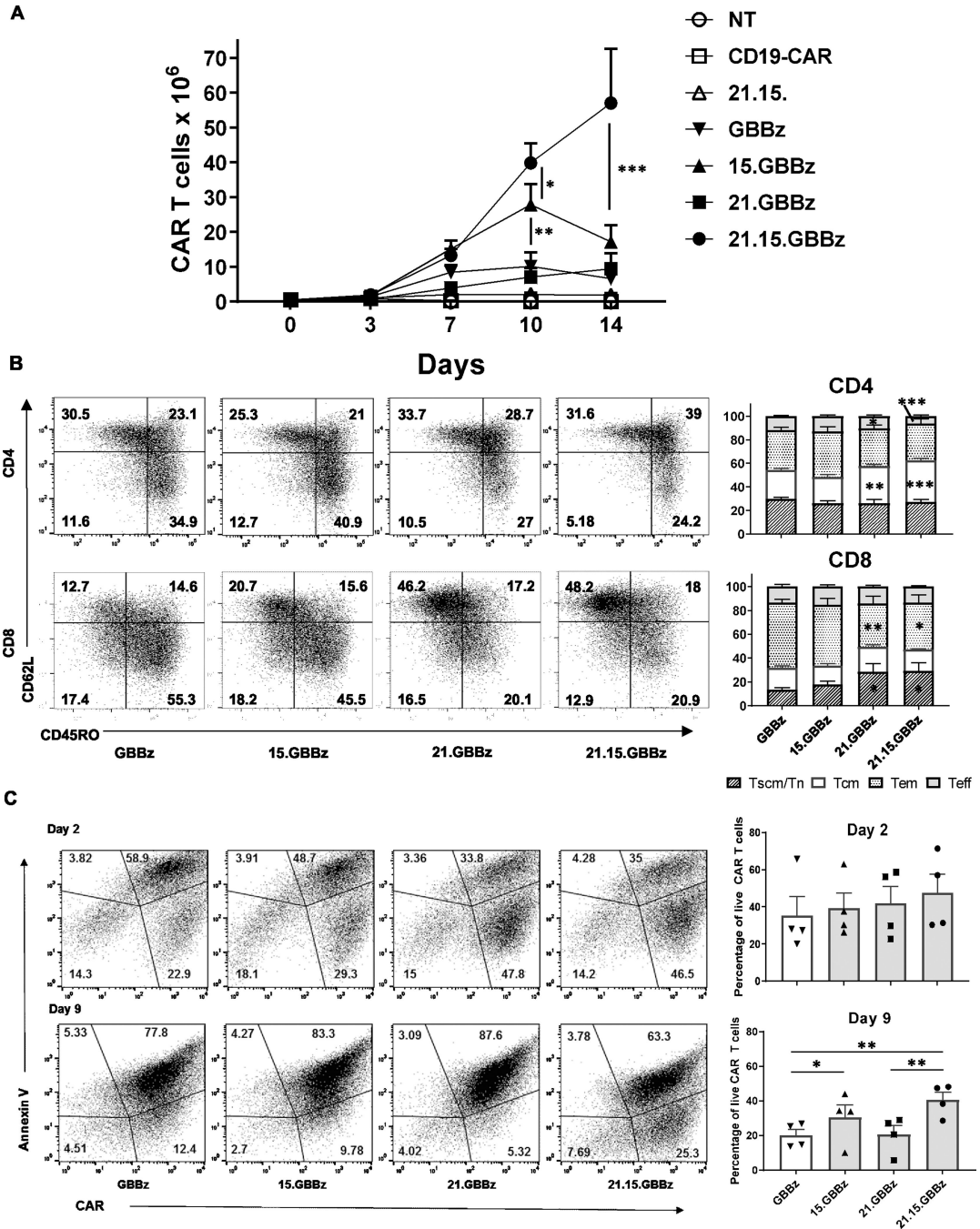


Figure 3. Co-expressing IL21 and IL15 enhanced expansion, enriched for less differentiated subsets, and reduced the apoptosis rate of GPC3-CAR T cells.

A) GPC3-CAR T cells were co-cultured with HCC cells at a 1:1 ratio and re-plated every 3–4 days as indicated with fresh HCC cells in the absence of exogenous cytokines (mean \pm SEM, combined data from three independent experiments evaluating three donors). One-way ANOVA followed. **B)** Phenotype of GPC3-CAR T cells as measured by surface expression of CD45RO and CD62L after manufacture. Shown are representative flow plots and summary data for indicated CAR T cell groups (mean \pm SEM, combined data

from four independent experiments evaluating four donors, asterisks indicate significant differences from GBBz). T_{scm}/T_n : CD45RO⁻/CD62L⁺, T_{cm} : CD45RO⁺/CD62L⁺, T_{em} : CD45RO⁺/CD62L⁻, T_{eff} : CD45RO⁻/CD62L⁻. **C**) GPC3-CAR T cells were stimulated once (day 2) or three times (day 9) with HCC cells at a 1:1 ratio and rate of apoptosis was evaluated by staining for annexin V. Representative flow plots and summary bargraph for indicated CAR T cell groups (mean \pm SEM, combined data from four independent experiments evaluating four donors). Data in Figures 3B and 3C were analyzed using two-way ANOVA. * $p < 0.05$, ** $p < 0.01$, *** $p < 0.001$.

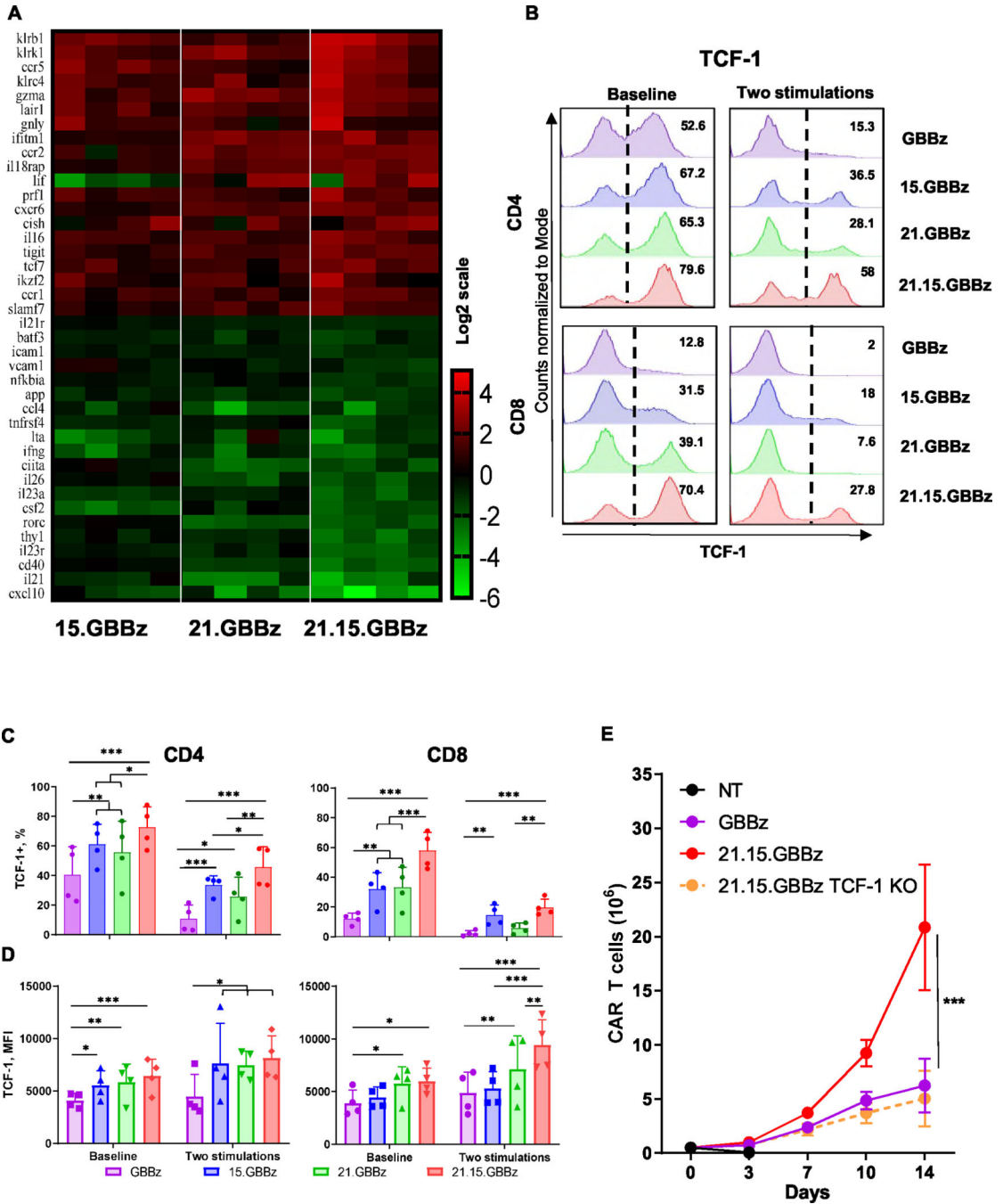


Figure 4. Co-expression of IL21 and IL15 altered global gene expression patterns in GPC3-CAR T cells and TCF-1 was maintained in CAR T cells co-expressing both IL15 and IL21.

A) Heat maps showing fold expression changes for top 20 genes with highest or lowest change in expression and reaching significance versus GBBz T cells (arranged with respect to 21.15.GBBz vs GBBz), as measured three days after stimulation with HCC cells (Four independent cocultures evaluating four independent donors, Nanostrings performed as a single batch). **B-D)** TCF-1 protein expression within CD4⁺ and CD8⁺ GPC3-CAR T cells as measured by intracellular flow cytometry. A representative histogram (**B**) and combined

results showing percentage (**C**) and mean fluorescence intensity (MFI, **D**) of TCF-1+ cells (mean + SD, combined data from four independent experiments evaluating four independent donors). Two-way ANOVA, * p<0.05, ** p<0.01, ***p<0.001. **E**) Expansion of indicated GPC3-CAR T cell populations with or without TCF-1 KO after stimulation with GPC3+ tumor cells. (Mean, ± SD, combined results from three independent experiments evaluating five independent donors, Student's T-test: p< 0.001).

Author Manuscript

Author Manuscript

Author Manuscript

Author Manuscript

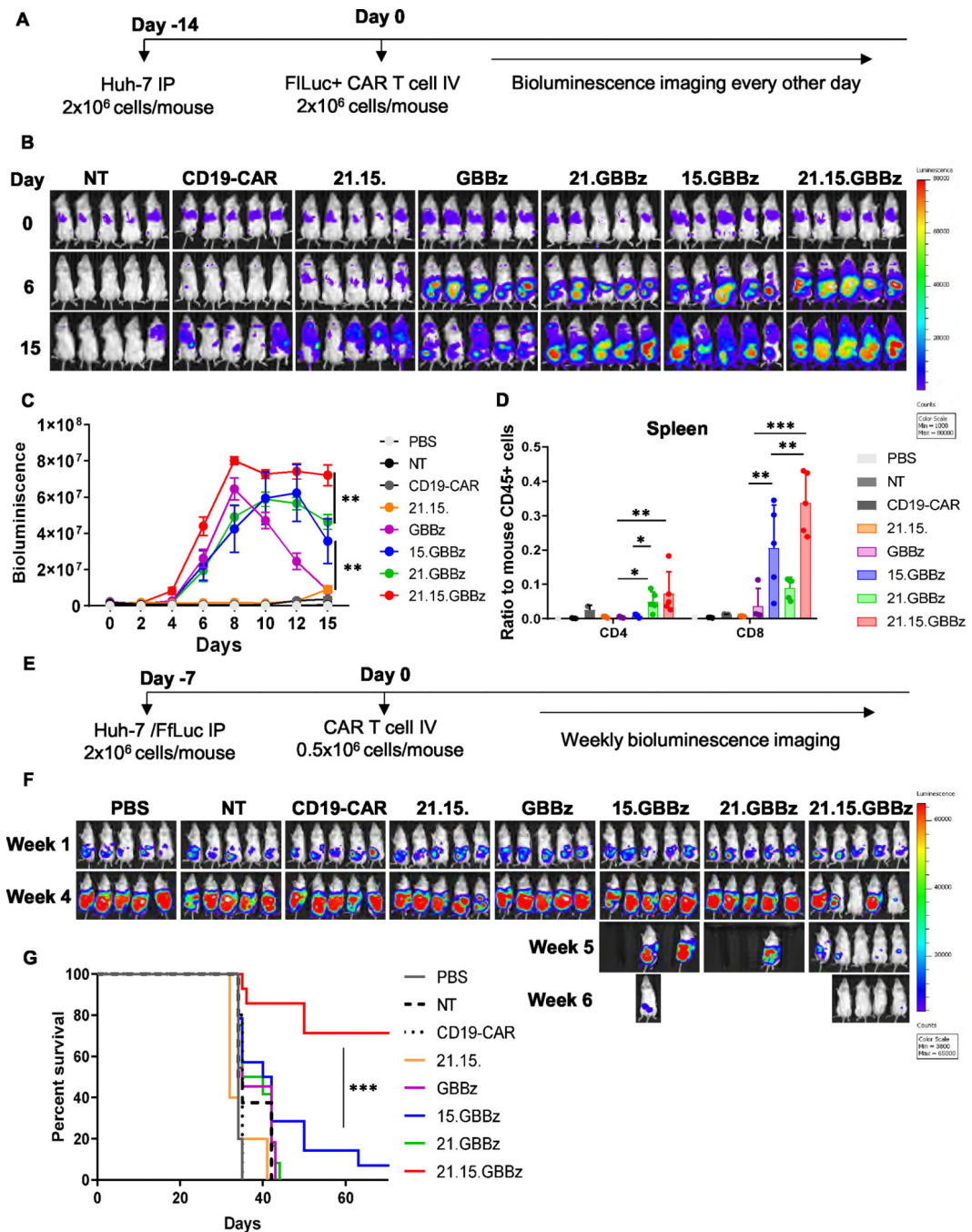


Figure 5. Co-expression of IL15 and IL21 enhanced *in vivo* expansion, persistence, and antitumor activity of GPC3-CAR T cells.

A) Schematic of *in vivo* evaluation scheme for GPC3-CAR T cell persistence. NSG mice were injected with 2×10^6 Huh-7 cells followed by 2×10^6 Ffluc+ CAR T cells two weeks later. **B)** Monitoring of bioluminescent GPC3-CAR T cells at indicated time points post-injection. **C)** GPC3-CAR T cell bioluminescence counts (mean \pm SEM) over experimental time course. **D)** Ratio of CD4⁺ and CD8⁺ GPC3-CAR T cells relative to mouse CD45-expressing cells in splenic tissue on day 18 as measured by flow cytometry. (mean

+ SD, one representative of two independent experiments, n=8–10 / GPC3 CAR T group). **E)** Schematic of *in vivo* evaluation scheme for GPC3-CAR T cell antitumor activity. NSG mice were injected with 2×10^6 Huh-7/FfLuc cells followed by 0.5×10^6 CAR T cells on day 7. **F)** Weekly monitoring of bioluminescent Huh-7 tumor cells. **G)** Kaplan-Meier survival analysis of tumor-bearing mice pictured in **(F)** Data in Figures 5C and 5D were analyzed using one-way ANOVA. Combined results from two independent experiments 11–14 animals per GPC3-CAR T cell groups. Survival was estimated by the Kaplan-Meier method and compared by the Gehan-Breslow-Wilcoxon test. * $p < 0.05$, ** $p < 0.01$, *** $p < 0.001$.

Author Manuscript

Author Manuscript

Author Manuscript

Author Manuscript